Int. J. Ion Mobil. Spec.
https://doi.org/10.1007/s12127-017-0223-x

ORIGINAL RESEARCH

An open source ion gate pulser for ion mobility spectrometry

Luke Garcia[1] · **Carolyn Saba**[1] · **Gabriela Manocchio**[1] · **Gordon A. Anderson**[2] · **Eric Davis**[1] · **Brian H. Clowers**[3]

Received: 2 October 2017 / Accepted: 5 October 2017

Abstract Excluding the ion source, an ion mobility spectrometer is fundamentally comprised of drift chamber, ion gate, pulsing electronics, and a mechanism for amplifying and recording ion signals. Historically, the solutions to each of these challenges have been custom and rarely replicated exactly. For the IMS research community few detailed resources exist that explicitly detail the construction and operation of ion mobility systems. In an effort to address this knowledge gap we outline a solution to one of the key aspects of a drift tube ion mobility system, the ion gate pulser. Bradbury-Nielsen or Tyndall ion gates are found in nearly every research-grade and commercial IMS system. While conceptually simple, these gate structures often require custom, high-voltage, floating electronics. In this report we detail the operation and performance characteristics of a wifi-enabled, MOSFET-based pulser design that uses a lithium-polymer battery and does not require high voltage isolation transformers. Currently, each output of this circuit follows a TTL signal with ~20 ns rise and fall times, pulses up to +/− 200 V, and is entirely isolated using fiber optics. Detailed schematics and source code are provided to enable continued use of robust pulsing electronics that ease experimental efforts for future comparison.

Keywords Ion mobility spectrometry · Ion gating · Open source hardware

Introduction

Early experiments with ion mobility spectrometry focused largely on the fundamentals of gas-phase ionization mechanisms and ion chemistry but finds contemporary applications across a range of fields. In addition to its more recent use as a bioanalytical tool coupled with mass spectrometry, atmospheric pressure drift tube IMS is used extensively for the detection of explosives, drugs, and chemical warfare agents [1–5]. Compared to instruments requiring extensive power or vacuum pumping requirements, commercial IMS systems are often low-cost, rapid, portable, and, provided the correct ion chemistry, quite sensitive [6]. In general, a drift time IMS relies on five fundamental principles or actions for a complete instrument: a method of sample introduction, sample ionization, means to modulate the ion population (i.e. ion gating) into a drift region, ion separation by gas-phase mobility coefficients, and detection. Each of these aspects of IMS have been addressed in the literature in depth. Ionization mechanisms and sources vary broadly with notable efforts using non-radioactive sources [7], electrospray ionization [8, 9], and matrix assisted laser desorption [10, 11]. Ion separation within the drift space has been addressed from an experimental and theoretical perspective and through theoretical modeling of the drift separation [12–14]. Detection of ions is possible using a range of approaches with Faraday plates and mass spectrometers being the most common approaches [15]. It worthy to note that though these two approaches remain dominant for a host of reasons, opportunities exists to exploit other characteristics for detection [16]. Though variations exist for all of these different components the means by which ions are gated is relatively consistent.

Electronic supplementary material The online version of this article (https://doi.org/10.1007/s12127-017-0223-x) contains supplementary material, which is available to authorized users.

✉ Brian H. Clowers
brian.clowers@wsu.edu

[1] Azusa Pacific University, Azusa, CA 91702, USA

[2] GAA Custom Engineering, Benton City, WA, USA

[3] Department of Chemistry, Washington State University, Pullman, WA 99164, USA

Published online: 24 October 2017

The options include either discrete pulsing of an ion source (e.g. laser desorption) or modulation of a continuous ion source via electrical or mechanical methods [17–20].

While ion gating is not a problem unique to IMS, as time of flight mass spectrometers occasionally use Bradbury Nielsen ion gates the effective gating of ions technologically challenges when discrete and accurate pulsing is required. IMS experiments typically pulse ions into the drift region at a frequency of 20–40 Hz, with a 50–200 μs gate open time at the start of each experiment. Thus, the ion gate must provide an ion pulse of consistent width and timing. As the efficiency of the separation of ions in the drift space fundamentally relies on the width of the initial pulse and thermal diffusion the ion gate is of central importance [14].

The most common method for ion introduction is through an electrostatic ion gate. The physical structures of these gates adopts one of two configurations. The Bradbury Nielsen (BN Gate) ion gate consists of parallel set of wires onto which a gating field may be introduced by biasing every other wire to a potential relative to the field in the vicinity of the gate [21, 22]. This creates an orthogonal electric field which prevents ions from moving through the gate region. Pulsing these wires to a referenced 0 V forces the gate into an "open" position, allowing ions to transit the space. However, the closing field of a BN gate creates a depletion region which reduces the ion signal and subsequent sensitivity. The second electric grid configuration found in ion mobility systems is the Tyndall ion gate.

A Tyndall gate consists of two, closely spaced grids of wires that serve to establish the stopping potential within the drift space [23]. As opposed to the BN gate where every other wire is positive or negative in polarity, the Tyndall gate uses the first gate with a positive bias and the second gate in a negative bias. The net result is the same; an orthogonal electric field which does not allow ions to pass. However, the space between the gates is finite and large when compared to the wire thickness of a BN gate, resulting in an increase to the gate depletion region effect. The Tyndall gate is often used as it is simpler to construct and maintain.

A field switching shutter, is a concept originally introduced by Blanchard et al. [24] that has been recently refined that that maintains a uniform potential separating the ionization region from the drift region of the IMS cell [19]. To achieve the ion gating effect the potential of the ionization source and region of the cell is often rapidly increased, driving ions over the potential "wall" formed by the shutter and into the drift region of the cell. This results in a decrease of the gate depletion region, and simplifies construction of the ion gate. However, the perturbation of the drift field caused by the field switch and limitations in the electronics used to create a field switching pulse have slowed the broad-scale adoption of this gating method [4, 19]. Regardless of the design, each ion gate described still suffers from a maximum ion gate transparency limited by the optical transparency of the grid. Work by Davila et al. illustrates these concepts by noting an overall decrease in ion current due to the impingement of ions onto the gate wires even when in the "open" state [23].

Attempts have also been made to create mechanical ion gates which do not depend on wire grids or pulsing signals to open the gate. These include rotating choppers wherein a hole in a spinning disk allows ions through only when space within the drift region [20]. This design eliminates the gate depletion region and water clustered ion leakage, but results in non-uniform introduction of ions into the drift region as the hole passes through the cell. With limited adoption of this technique, the majority of IMS systems rely on ion gate designs with the majority utilizing BN and Tyndall gates. However, these ion gates all rely on electronics that pulse floated voltages onto the grid structure relative to the reference voltage. Traditionally, these electronics have relied on custom-made, wire-wound isolation transformers to translate TTL signals into the high voltage pulsing needed to admit and stop ions entering the drift cell of an IMS. Such "gate controls" have remained either proprietary in nature or custom built from in-house electronics experts.

In an effort to address this knowledge and resource gap, we outline a traceable solution to the construction and operation of ion mobility spectrometers using modern off-the shelf components for an inexpensive solution to the gating of ions. This new, open-sourced gate pulser can be used with Bradbury-Nielsen or Tyndall ion gates and any TTL-level input for the pulsing scheme; including traditional drift time IMS and multiplexing methods such as Hadamard and Fourier transform gating schemes.

Experimental

Gases and reagents Ultra-high purity nitrogen, passed through a molecular sieve, was used as the drift gas throughout the experiment, with a flow rate of ~1.0 L/min. The primary analyte, 2,4-lutidine (Aldrich, Milwaukee, WI) was diluted to ~50 ppm in a 50/50 mixture of water (HPLC Grade, Fisher, Fair Lawn, NJ) and methanol (HPLC Grade, Fisher, Fair Lawn, NJ). This solution was placed into a standard 11 mm autosampler vial and sealed with a pre-pierced septum cap. This vapor introduction setup was placed into a 20 mL scintillation vial entrained into the source gas flow (see below).

IMS cell The IMS cell utilized in this work has been described previously [25]. In short, the cell consisted of 22 stainless steel rings separated by alumina spacers, resulting in an 11.4 cm drift cell. The rings were held in an aluminum heater casing capable of maintaining the temperature of the drift cell at a constant 180 °C. Drift gas was also heated to 180 °C and introduced at the end of the drift cell via a showerhead design. Carrier gas flow was directed through the headspace of a 20 mL scintillation vial and swept into the IMS cell via a

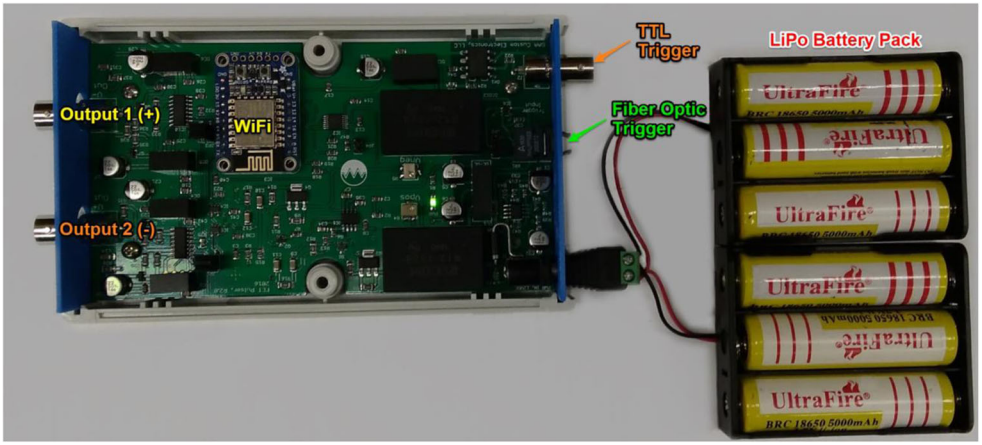

Fig. 1 Photo of the operational FET pulser including a WiFi module which controls the voltage on Outputs 1 and 2 that alters between and open and closed state depending upon the levels of the input trigger. The trigger can be input either through a TTL pulse or a fiber optic port. Using the LiPo battery pack displayed the system can operate for ~8 h while responding to a 1 kHz input signal and +/− 25 V output on the gate leads

capillary placed within the ionization region. A ^{63}Ni (10 mCi) foil situated on a screen in the first ring of the IMS tube provided ionization of gas-phase analytes. Leads connected to the respective wire sets on the Bradbury-Nielsen ion gate were exposed to allow rapid switching between the traditional gate pulser and the FET design. Software control handling data acquisition and output timing signals was programmed in LabVIEW (National Instruments, Austin, Texas) and detailed previously [26].

Pulser electronics The traditional pulser used in many of the prior atmospheric pressure studies conducted at Washington State University was based upon an optically isolated analog circuit relying upon a custom, wire-wound isolation transformer to translate 110 V AC power into the floated circuit capable of outputting +/−100 V relative to a reference voltage. This system contains one reference input, provided by the resistive divider of the stacked ring IMS, and two outputs going to the respective wire sets within the ion gate.

In contrast to the traditional configuration, the new pulser detailed in this report is based upon a set of off-the-shelf components that are readily available does not require any custom hardware. To achieve effective ion gating, the pulser produces complementary output pulses (positive and negative output channels) using FET push-pull output drivers to form a switch. This switch connects the output of the pulser to ground reference or to its supply voltage, thus switching the output between these two states. Two N-channel FETs and an Analog Devices ADUM3223 isolated half bridge gate driver, used to drive the FET gates, form the switch. Two of these switch configurations are used one for each of the complementary outputs. The ADUM3223 provides full isolation and is powered using isolated DC-to-DC converters; this allows identical circuits for the positive and negative output channels. The positive and negative supply voltages are adjustable from 0 to 200 and −200 V respectively. The supply voltages are generated with DC-to-DC converters and simple linear regulators are used to develop the adjustable voltages for each of the FET switches. These adjustable supplies provide the drive voltage to the FET switches and

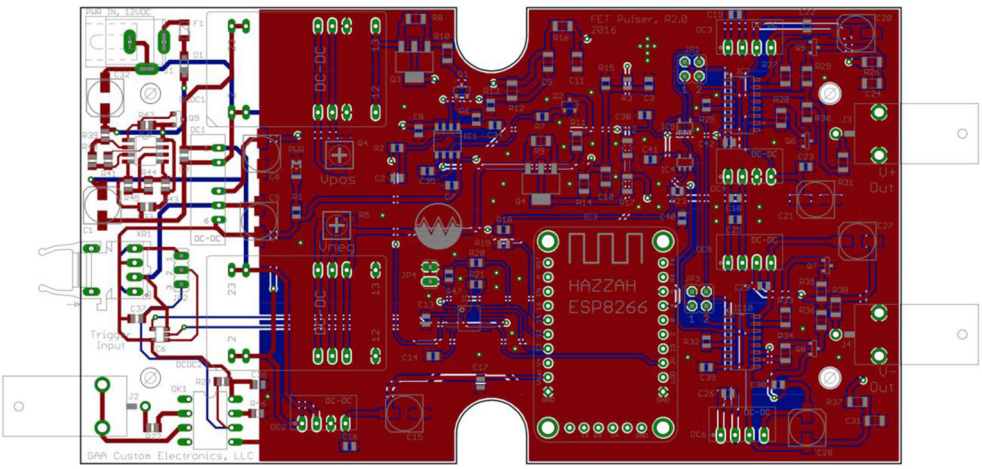

Fig. 2 Unpopulated board outline of the FET pulser. This schematic along with the information required to construct and operate the system can be found in the supplementary material

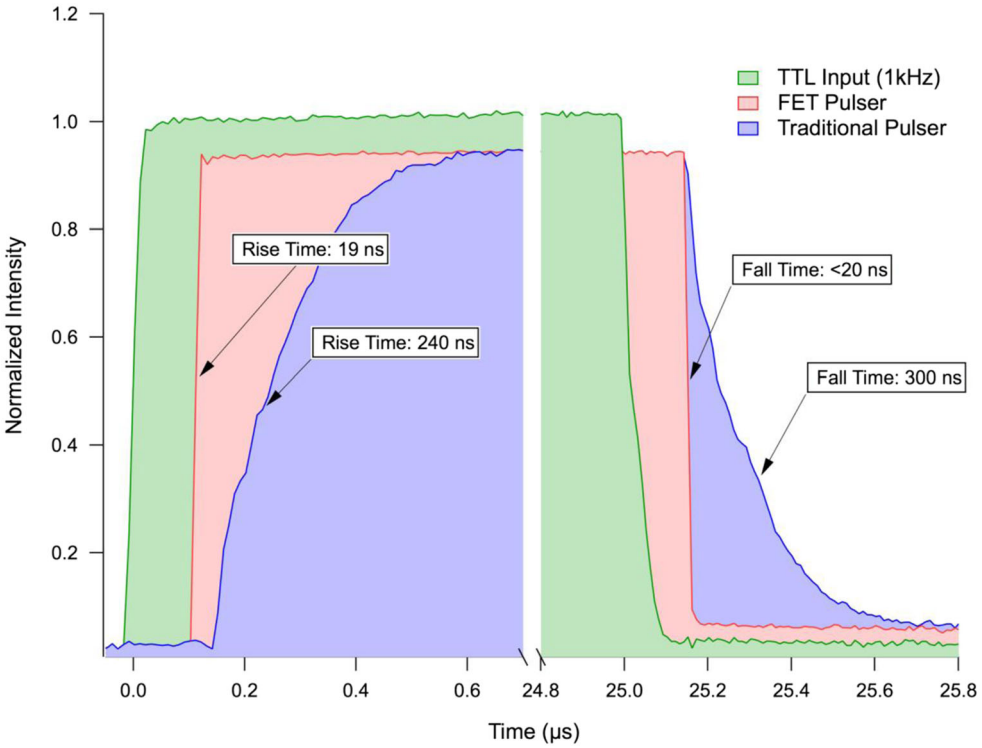

Fig. 3 Comparative performance of the newly designed FET pulser illustrates improved rise and fall times when tracking a 1 kHz input TTL signal with a 50% duty cycle. The +/− voltage for both the traditional WSU pulser and the newer design was set to 50 V for each output. The performance of the custom, wire-wound transformer, illustrates rise and fall times that approach a few hundred nanoseconds where the newer solid-state design yielded pulse transitions in under 20 ns

are controlled using an ESP8266 wireless controller. This controller provides a WiFi interface as well as digital IO and serial interface to a digital to analog converter used to set the output pulse voltages. The WiFi interface allows full control and monitoring of the system, this enables powering the system using batteries and floating at high voltages while still having full control of the parameters. The ESP8266 is programed using the Arduino interactive development environment and the code is written is C++ (See Supplementary Information for source code and input commands). It should be noted that the WiFi interface allows the user to alter the gate output voltage and characteristics but is not required at the start of each operation. Once the desired settings are saved, upon applying power the same settings are reloaded. To accommodate a range of applications and float voltages, two options are provided to trigger the pulser, an optically-isolated 0 to 5-V input trigger or a fiber optic input to provide higher voltage isolation. The pulser requires 11-12 V DC as an input with a current draw of approximately 0.25 A. For the experiments conducted in this report 3.7 V, 5000 mAh, 18,650 lithium polymer (lipo) batteries were used. These rechargeable batteries contain an internal circuit that prevents excessive battery drain to extend battery lifetime and minimize potential hazards that result from lipo battery overuse.

Results and discussion

To evaluate the performance of the open-source pulser relative to the traditional legacy pulser as series of experiment were conducted emphasizing pulse shape characteristics, resulting ion mobility peak shape, and battery lifetime. Before describing the results from the experiments, it is worth examining the the images in Figs. 1 and 2. The first figure depicts the the pulser connected the the lithium-polymer (lipo) battery pack. This power pack comprises of two individual battery packs that each contain three 18,650 batteries. This combined battery pack yielded ~11.1 VDC which is sufficient to drive the FET pulser. Figure 2 contains an image of the unpopulated FET pulser board and the raw printed circuit board files can be examined in greater detail using the materials supplied in the Supplemental Information.

In an effort to assess the performance characteristics of the newly designed pulser and the legacy gate driver the outputs of each pulser relative to the input pulse were examined using a 300 MHz oscilloscope and appropriate probes. After setting both pulsers to identical gate closing voltages (+/− 25.0 V), a TTL (0–5 VDC) input pulse train was supplied at 1 kHz at a 50% duty cycle to each of respective pulsers and the outputs measured. As illustrated in Fig. 3, the FET pulser demonstrated rise and fall times under 20 ns, while the legacy pulser required 240 ns to reach the fully “open” state and 300 ns to fully close. To ensure the appropriate comparison the signal from the function generator was split into both gate pulsers simultaneously and the input pulse (green) and output pulses (red and blue) were monitored via an oscilloscope simultaneously. Though both pulsers responded on time scales that vastly exceed the drift velocity and diffusional spread of ion packets in a mobility cell, Fig. 3 suggest that the newer FET

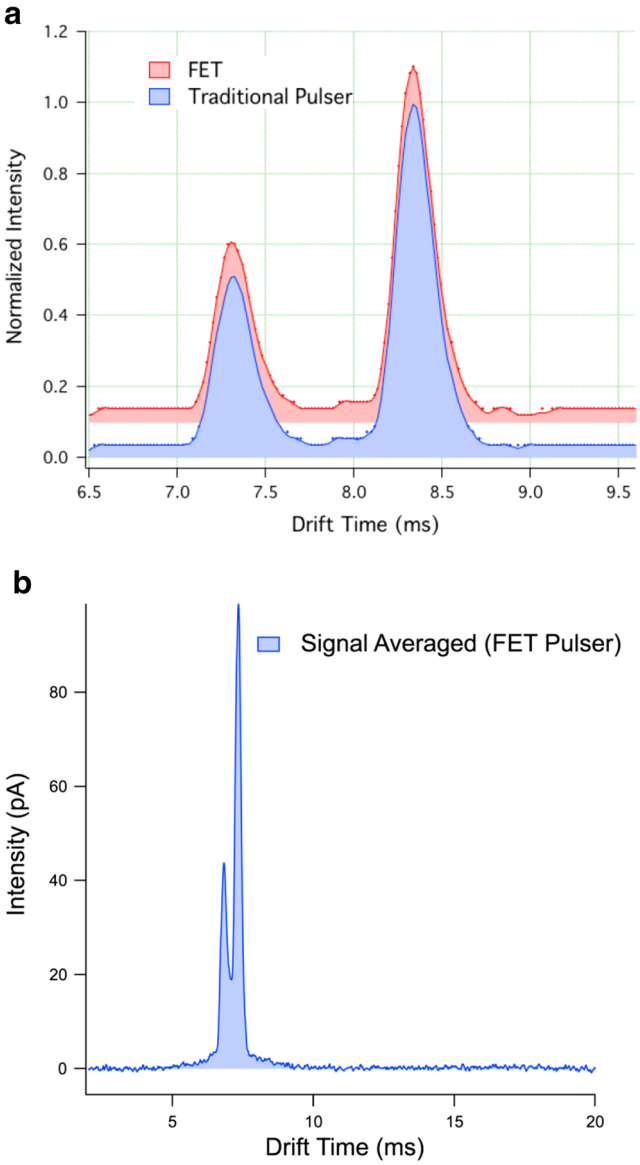

Fig. 4 **a** Overlaid spectra for 2,4-lutidine peak, at a reference voltage of 4445 V with an applied gate voltage of +/− 27.0 V for both the FET and traditional pulsers. To minimize any capacitive loading between the two gate pulse circuits the reference leads of both pulsers were simultaneously connected to the ion gate. **b** Using a 150 μs gate pulse width as an input, the spectrum highlights the reactant ion peaks obtained using the new FET pulser

pulser yields ion gating waveforms that are closer to the ideal than the traditional pulser.

When considering previous efforts by Puton et al. to model the ion populations immediately after entering the drift cell, ion gate non-idealities establish a situation where the front and rear of the ion packet experience an electric field gradient as the gate is not fully open or fully closed within this time [22]. Moreover, non-idealities in ion gating behavior are at times difficult to capture but can hinder attempts to accurately model peak distributions. Another aspect of the pulse train comparison experiment worth considering is the response time of the pulser relative to the input TTL signal. The FET pulser has shown that it was capable of responding to the input signal more rapidly than the legacy pulser (Fig. 3). With the IMS experiment often occurring on the millisecond time scale, this difference in timing is quite negligible as the delay is on the order of 100 s of nanosecond. Nevertheless, this type of behavior may be worth considering for lower pressure systems where drift times can be on the microsecond timescale.

Analytically, the primary concern when evaluating a new set of pulsing electronics is whether the system produces the expected ion pulse shapes at the detector. Using the sample introduction system detailed in the experimental section, we examined the peak shapes resulting from the FET pulser relative to the traditional driver. Figure 4**a** demonstrates a comparison of an IMS spectrum of 2,4-lutidene using the analog pulser (blue) and the FET pulser (red). In this experiment, the reference lead from both gate pulsers were connected to the IMS cell to avoid any electric field changes due to the pulser electronics. Both pulsers were set to a gate close voltage of +/−27.0 V and verified with a multimeter prior to applying high voltage to the drift cell. Only the gate pulsing leads were changed between the two spectra. Under these conditions the resulting spectra closely resemble one another and were not statistically different. It should be noted that the measured drifts times provide yielded reduced mobilities of 1.96 $cm^2\ V^{-1}\ s^{-1}$ for both the new pulser and the traditional pulser.

In a subsequent experiment the open-source gate pulser was compared to yet a second legacy gate driver in operation at Washington State University in its capacity to function in experiments requiring multiple, high-frequency gating events (i.e. ion gate multiplexing. Fig. 5 illustrates a comparison between the FET pulser and the legacy gate driver when conducting a single gate Fourier transform experiment using the ion mobility-time of flight mass spectrometer as detailed by Davis and Clowers [27, 28]. These data illustrate that new pulser is also capable of performing multiplexing experiments which for the basis of many modern IMS experiments.

A core departure of the new pulser relative to the the traditional pulser at WSU is the fact that the newer system requires an external, isolated power supply or a battery pack. This design choice was made as it is eases floating efforts often necessary for drift tube IMS experiments. Moreover, by floating with a battery pack any issues that arise during a prototyping effort related to electrical breakdown minimize damage. With ready access of rechargeable lipo batteries implementation of the battery configuration is quite flexible. Using the battery pack shown in Fig. 1 the newly designed system was floated was test up to float voltages of 10 kV without issue. Higher voltages were not tested but it is anticipated that the limiting factor influencing the maximum float voltage is the fiber optic cable delivering the signal for the trigger pulse. Using the conditions shown for the Fig. 3 (i.e.

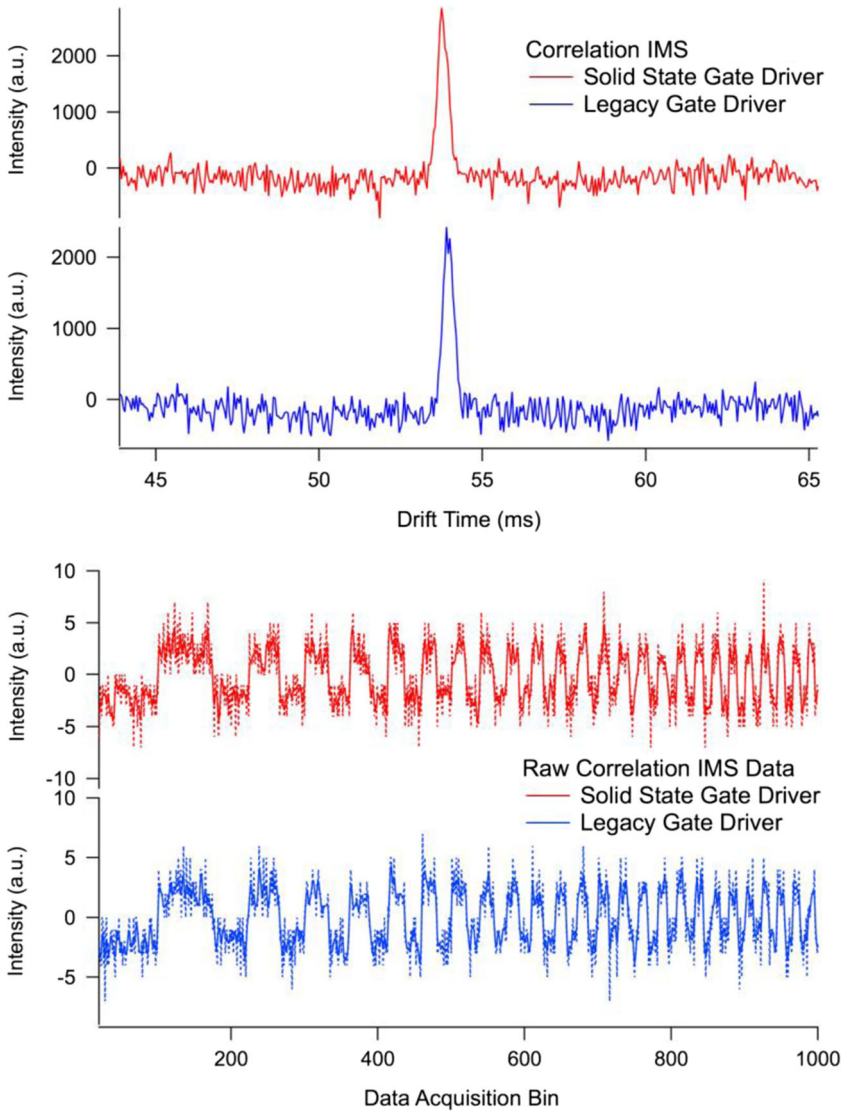

Fig. 5 Comparison of the frequency swept waveforms obtained with the legacy and new ion gate pulser using an ion mobility time of flight mass spectrometer. The top set of mobility peaks correspond to the Fourier transforms of the bottom two raw data sets. No smoothing or additional processing was applied to the data sets shown

a 1 kHz, 50% duty cycle waveform at +/− 25 VDC) the the FET pulser was able to operate continuously for ~550 min (just shy of initial calculations). In our hands we routinely have two sets of batteries on hand with one in operation and the other charging or charged at all times. The ability to operate close to 10 h without intervention is usually sufficient for most mobility experiments.

Conclusions

Presented herein are the designs for an open-source, relatively inexpensive gate pulser constructed with modern, off-the-shelf components that provides superior gate pulsing characteristics and identical spectral details to traditional designs. Specifically, the new pulser demonstrated superior rise and fall times when compared to the legacy designs. While the rise and fall times improvements did not impact the spectral characteristics for the ion gate and IMS systems used in this effort, progress towards high resolution instruments and investigations relying upon a known gate impulse function could benefit from well-defined peak shapes. This latter point is especially relevant to efforts to minimize transform artifacts when performing multiplexed ion mobility experiments. It is also worthy to note that the new gate pulser is controlled wirelessly and its reliance on rechargeable battery power does not place upper limits on its float voltage level. This new open-source gate pulser is available to the community with all plans, designs, and firmware available in the supplementary material.

Acknowledgements ED and students from Azusa Pacific University were supported by the National Science Foundation (CHE-1507155) and BHC would like to acknowledge support from the NSF (CHE-1506672).

References

1. Daum KA, Atkinson DA, Ewing RG (2002) The role of oxygen in the formation of TNT product ions in ion mobility spectrometry. Int J Mass Spectrom 214:257–267
2. Ewing RG, Atkinson DA, Eiceman GA, Ewing GJ (2001) A critical review of ion mobility spectrometry for the detection of explosives and explosive related compounds. Talanta 54:515–529
3. Eiceman GA, Nazarov EG, Stone JA (2003) Chemical standards in ion mobility spectrometry. Anal Chim Acta 493:185–194
4. Chen C, Tabrizchi M, Wang W, Li H (2015) Field switching combined with Bradbury-Nielsen gate for ion mobility spectrometry. Anal Chem 87:7925–7930
5. Mäkinen MA, Anttalainen OA, Sillanpää MET (2010) Ion mobility spectrometry and its applications in detection of chemical warfare agents. Anal Chem 82:9594–9600
6. Eiceman GA, Karpas Z, Hill HH Jr (2013) Ion Mobility Spectrometry, 3rd edn. CRC Press, Boca Raton, pp 1–20
7. Gunzer F, Ulrich A, Baether W (2010) A novel non-radioactive electron source for ion mobility spectrometry. Int. J. Ion Mobil. Spec. 13:9–16
8. Wittmer D, Chen YH, Luckenbill BK, Hill HH (1994) Electrospray ionization ion mobility spectrometry. Anal Chem 66:2348–2355
9. Hoaglund-Hyzer CS, Clemmer DE (2001) Ion trap/ion mobility/quadrupole/time-of-flight mass spectrometry for peptide mixture analysis. Anal Chem 73:177–184
10. Fenn LS, Kliman M, Mahsut A, Zhao SR, McLean JA (2009) Characterizing ion mobility-mass spectrometry conformation space for the analysis of complex biological samples. Anal Bioanal Chem 394:235–244
11. Gillig KJ, Ruotolo B, Stone EG, Russell DH, Fuhrer K, Gonin M, Schultz AJ (2000) Coupling high-pressure MALDI with ion mobility/orthogonal time-of-flight mass spectrometry. Anal Chem 72:3965–3971
12. Spangler GE (2002) Expanded theory for the resolving power of a linear ion mobility spectrometer. Int J Mass Spectrom 220:399–418
13. Kirk AT, Bakes K, Zimmermann S (2017) A universal relationship between optimum drift voltage and resolving power. Int J Ion Mobil Spec:1–5
14. Siems WF, Wu C, Tarver EE, Hill HH Jr, Larsen PR, McMinn DG (1994) Measuring the resolving power of ion mobility spectrometers. Anal Chem 66:4195–4201
15. Eiceman GA, Karpas Z, Hill HH Jr (2013) Ion mobility spectrometry. CRC Press, Third Edition
16. Davis EJ, Siems WF, Hill HH Jr (2012) Radiative ion-ion neutralization: a new gas-phase atmospheric pressure ion transduction mechanism. Anal Chem 84:4760–4767
17. Du Y, Wang W, Li H (2012) Bradbury-Nielsen-gate-grid structure for further enhancing the resolution of ion mobility spectrometry. Anal Chem 84:5700–5707
18. Brunner T, Mueller AR, O'Sullivan K, Simon MC, Kossick M, Ettenauer S, Gallant AT, Mané E, Bishop D, Good M, Gratta G, Dilling J (2012) A large Bradbury Nielsen ion gate with flexible wire spacing based on photo-etched stainless steel grids and its characterization applying symmetric and asymmetric potentials. Int J Mass Spectrom 309:97–103
19. Kirk AT, Zimmermann S (2014) Bradbury-Nielsen vs. Field switching shutters for high resolution drift tube ion mobility spectrometers. Int J Ion Mobil Spec 17:131–137
20. Zhou L, Collins DC, Lee ED, Rockwood AL, Lee ML (2007) Mechanical ion gate for electrospray-ionization ion-mobility spectrometry. Anal Bioanal Chem 388:189–194
21. Kai N, Jingran G, Guangli O, Yu L, Quan Y, Xiang Q, Xiaohao W (2014) A simple template-based transfer method to fabricate Bradbury-Nielsen gates with uniform tension for ion mobility spectrometry. Rev Sci Instrum 85:085107
22. Puton J, Knap A, Siodłowski B (2008) Modelling of penetration of ions through a shutter grid in ion mobility spectrometers. Sens Actuators B Chem 135:116–121
23. Davila SJ, Hadjar O, Eiceman GA (2013) Ion profiling in an ambient drift tube-ion mobility spectrometer using a high pixel density linear array detector IonCCD. Anal Chem 85:6716–6722
24. Blanchard WC, Nazarov EG, Carr J, Eiceman GA (2017) Ion Injection in a Mobility Spectrometer using Field Gradient Barriers, i.e. Ion Wells
25. Davis EJ, Williams MD, Siems WF, Hill HH Jr (2011) Voltage sweep ion mobility spectrometry. Anal Chem 83:1260–1267
26. Davis EJ, Clowers BH, Siems WF, Hill HH (2011) Comprehensive software suite for the operation, maintenance, and evaluation of an ion mobility spectrometer. Int. J. Ion Mobil. Spec. 14:117
27. Clowers BH, Siems WF, Yu Z, Davis AL (2015) A two-phase approach to Fourier transform ion mobility time-of-flight mass spectrometry. Analyst 140:6862–6870
28. Davis AL, Liu W, Siems WF, Clowers BH (2017) Correlation ion mobility spectrometry. Analyst 142:292–301